PAPER

A systematic study of solvation structure of asymmetric lithium salts in water

To cite this article: Lingzhe Fang *et al* 2024 *Nanotechnology* **35** 365402

IOP Publishing Nanotechnology
Nanotechnology 35 (2024) 365402 (6pp) https://doi.org/10.1088/1361-6528/ad4ee7

A systematic study of solvation structure of asymmetric lithium salts in water

Lingzhe Fang[1,3], Huong Nguyen[1,3], Rena Gonzalez[1] and Tao Li[1,2,*]

[1] Department of Chemistry and Biochemistry, Northern Illinois University, DeKalb, IL 60115, United States of America
[2] Chemistry and Material Science Group, X-ray Science Division, Argonne National Laboratory, Lemont, IL 60439, United States of America

E-mail: tli4@niu.edu

Received 8 January 2024, revised 17 April 2024
Accepted for publication 22 May 2024
Published 19 June 2024

Abstract

Aqueous electrolytes are promising in large-scale energy storage applications due to intrinsic low toxicity, non-flammability, high ion conductivity, and low cost. However, pure water's narrow electrochemical stability window (ESW) limits the energy density of aqueous rechargeable batteries. Water-in-salt electrolytes (WiSE) proposal has expanded the ESW to over 3 V by changing electrolyte solvation structure. The limited solubility and WIS electrolyte crystallization have been persistent concerns for imide-based lithium salts. Asymmetric lithium salts compensate for the above flaws. However, studying the solvation structure of asymmetric salt aqueous electrolytes is rare. Here, we applied small-angle x-ray scattering (SAXS) and Raman spectroscope to reveal the solvation structure of imide-based asymmetric lithium salts. The SAXS spectra show the blue shifts of the lower q peak with decreased intensity as the increasing of concentration, indicating a decrease in the average distance between solvated anions. Significantly, an exponential decrease in the d-spacing as a function of concentration was observed. In addition, we also applied the Raman spectroscopy technique to study the evolutions of solvent-separated ion pairs (SSIPs), contacted ion pairs (CIPs), and aggregate ions (AGGs) in the solvation structure of asymmetric salt solutions.

Supplementary material for this article is available online

Keywords: SAXS, water in salt, Raman spectroscopy, solvation structure

1. Introduction

Aqueous electrolytes with intrinsic low toxicity, non-flammability, higher ion conductivity and low total cost demonstrate significant potential for large-scale energy storage applications [1–3]. However, the existence of hydrogen and oxygen evolution leads to the narrow electrochemical stability window (ESW, 1.23 V) of pure water, which compromises the energy density of aqueous rechargeable batteries [4–7]. Suo *et al* proposed the concept of water-in-salt electrolytes (WiSE), where the weight and volume of salt both exceed that of water in 21 m (mol kg^{-1}) lithium bis(trifluoromethane sulfonyl)imide (LiTFSI) electrolyte, thereby expanding ESW to over 3 V [8]. Water molecules and $TFSI^-$ anion in the WiSE take part in the primary solvation sheath of Li^+, which profoundly affect the physicochemical properties of WiSE [9, 10]. The unique Li ion transport mechanisms in WiSE have been proposed despite the large macroscopic viscosity of WiSE [11, 12]. More importantly, as anions have more positive redox potentials than water, the solid electrolyte interphase (SEI) is predominantly derived from anion reduction in WiSE

[3] These authors contributed equally.
[*] Author to whom any correspondence should be addressed.

[13–15]. The stable anion-derived SEI and absence of free water prevent the hydrogen evolution reaction (HER) on the anode [16, 17]. Therefore, anion plays a vital role in the high round-trip energy efficiency and cyclability of high-voltage aqueous rechargeable batteries.

Of all the reported anions, organic imide anions are intensively studied [18–21]. The bulky imide anions with weakly Lewis basic feature effectively diminish water volume and promote the Li^+-water solvation structure [20]. However, the limited solubility of imide-based salts in water hinders their potential for further advancement. Ko *et al* found that the asymmetric salts in water are more soluble than symmetric salts, which makes them more suitable for the WiSE regime [22]. They enormously widened the ESW to 5 V by mixing asymmetric ion $N(SO_2CF_3)(SO_2C_2F_5)$(PTFSI) and symmetric ion TFSI with a 55.5 m concentration in water. Another concern is the low-temperature performance of aqueous batteries. WiSE approaches the salt solubility limit, leading to a tendency of crystallization during long-term cycling or operating at low temperatures [17]. Kühnel *et al* proposed the introduction of asymmetric imide anion to strengthen the electrolyte salt's intermolecular bonding, which effectively enables the WiSE stability at low temperature [23, 24]. Therefore, the systematic research of the solvation structure of asymmetric imide-based lithium salts in water benefits the understanding of WiSE.

Various characterization techniques have been applied to reveal the solvation structure of electrolytes, covering different scales and structural information. Infrared (IR) spectroscopy and Raman spectroscopy provide local information on the vibrations of chemical bonds of anions in the electrolyte. X-ray absorption spectroscopy (XAS) is used to explore the coordination environment of the elements of interest. However, the limitations of XAS restrict its use to studying atoms with high atomic numbers. Zhang *et al* applied XAS to investigate the coordination environment around Zn^{2+} in mixed $Zn(TFSI)_2$ and LiTFSI water-in-salt electrolytes [25]. They found that Zn^{2+} cations are primarily solvated by six water molecules in the first solvation shell without the presence of $TFSI^-$ anions. Distinct from the local information provided by IR/Raman spectroscopy and XAS, small-angle x-ray scattering (SAXS) offers statistical structural information at the nanometer scale by measuring electron density discontinuities in the target material [26–28]. Zhang *et al* investigated water-in-salt LiTFSI aqueous electrolytes using this technique [29]. Molecular dynamics (MD) simulations, producing x-ray structure factors at low q ranges, align well with x-ray total scattering data and SAXS structure factors. Therefore, SAXS data can be used as an effective method to validate the accuracy of the force field used in MD simulations. Consequently, SAXS is emerging as a pivotal tool in electrolyte characterization, which plays an irreplaceable role.

Here, we investigated the physicochemical properties of asymmetric lithium salts with different concentrations in water. By fixing one (fluorosulfonyl) (FS) side in lithium bis(fluorosulfonyl)imide (Li(FS-FS)I), extend chain lengths of the other side in FS-based lithium salts, such as (pentafluoroethane sulfonyl) (PFS) and (nonafluorobutane sulfonyl) (NFS), were studied. The SAXS spectra show the blue shifts of the lower q peak with decreased intensity as the increasing of concentration, indicating a decrease in the average distance between solvated anions. The increase in the population of anions and reduction of water molecules in highly concentrated solution induce the formation of FSI- networks, which is indicated by the formation of additional peaks at higher q value. Significantly, an exponential decrease in the d-spacing as a function of concentration was observed. In addition, we also applied Raman spectroscopy technique to study the evolutions of solvent-separated ion pairs (SSIPs), contacted ion pairs (CIPs), and aggregate ions (AGGs) in the solvation structure of asymmetric salt solutions.

2. Experimental section

2.1. Electrolyte preparation

Electrolytes with different concentrations were prepared by dissolving the lithium bis(fluoro sulfonyl)imide (LiFSI, 99.9%, Sigma-Aldrich), the lithium (fluoro sulfonyl)(pentafluoroethane sulfonyl)imide (Li(FS-PFS)I, >95%, Provisco CS) and the lithium (fluoro sulfonyl)(nonafluorobutane sulfonyl)imide (Li(FS-NFS)I, >95%, Provisco CS) in high purity water which conductivity is 18.2 MΩ × cm at 25 °C. All the electrolytes were prepared by molality (mole-salt in kg-solvent) used by abbreviated concentrations (1 m, 5 m, 10 m, 15 m, 20 m).

2.2. SAXS

SAXS experiments were measured at the Advanced Photon Source (APS) 12ID-B station of Argonne National Laboratory. The 2D SAXS data were collected on an Eiger 2S detector (DECTRIS Ltd) with an incident energy of 13 keV. The two-dimensional scattering images were radially averaged over all orientations to produce plots of scattered intensity I(q) versus scattering vector q, where $q = 4\pi \sin \theta/\lambda$. The scattering vector, q, was calibrated using silver behenate. The samples were loaded into 1.5 mm diameter quartz capillary tubes and sealed with epoxy for the SAXS measurement.

2.3. Raman spectroscopy

Raman spectra of the samples were collected at the GSECARS (Center for Nanoscale Materials, Argonne National Laboratory) with an excitation wavelength of 532 nm. The electrolytes were loaded into 1.5 mm diameter quartz capillary tubes and sealed with epoxy.

3. Results and discussion

3.1. SAXS results

We conducted SAXS measurements on LiFSI, Li(FS-PFS)I, and Li(FS-NFS)I with the increasing concentration, as illustrated in figure 1. As the concentration of Li(FS-FS)I in water increases, the Peak a shifts to a higher q value, suggesting the

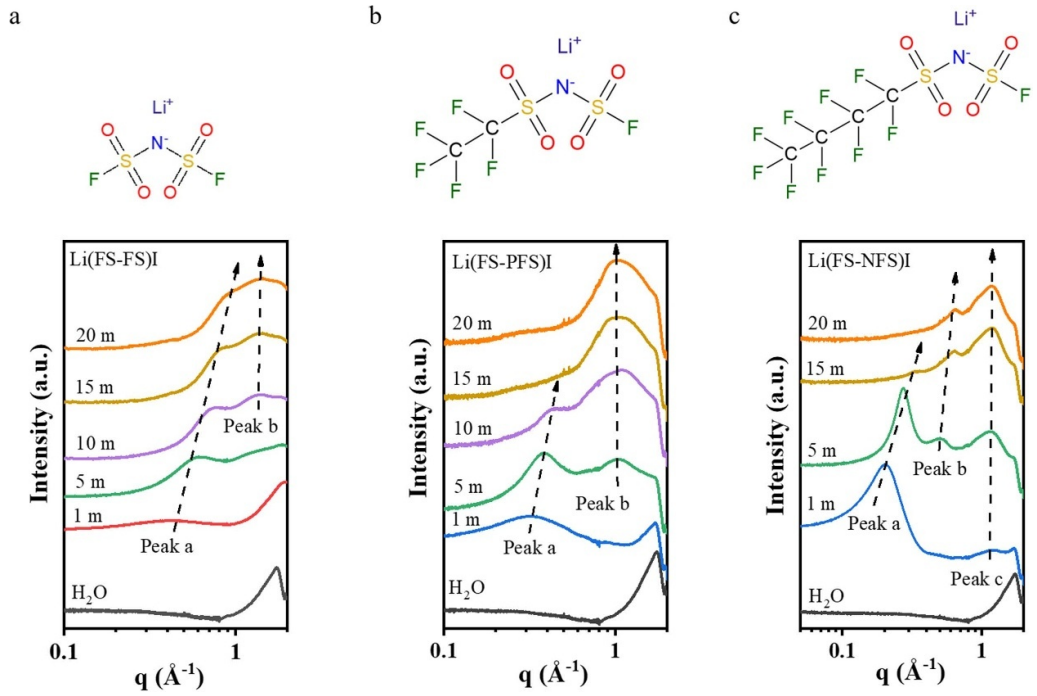

Figure 1. Molecular structure and corresponding SAXS profiles of (a) Li(FS-FS)I, (b) Li(FS-PFS)I, and (c) Li(FS-NFS)I aqueous solutions with different concentrations.

decreasing of the average distance between solvated FSI ions. This phenomenon can be ascribed to the heightened inclination of FSI anions to displace free water molecules from the outermost layer, consequently resulting in a diminished separation distance between solvated FSI anions. Interestingly, the Peak b located at higher q value appears as the concentration higher than 5 m. The increase in the population of FSI anions and reduction of water molecules in highly concentrated water solutions induce the formation of FSI^- networks. Different from the position changes of Peak a, the Peak b position remains unchanged as the concentration further increases. Compared with the symmetric Li(FS-FS)I salt, two Peaks can also be observed in aqueous solution of asymmetric Li(FS-PFS)I salt (figure 1(b)). Significantly, the Peak a shifts to higher q but disappears at high concentrations (15 m and 20 m), which is consistent with the observed phenomenon in symmetric Li(TFS-TFS)I salt solution. The decrease in the Peak a intensity, accompanied by the emergence and intensification of Peak b indicate that the FSI-solvated structure gradually disappears and the (FS-PFS)I anion networks form, respectively. A reduction in the relative abundance of water molecules in a concentrated solution causes solvation structure changes, which is highly related to the electrochemical performance. As the chain expands, the Li(FS-NFS)I water solutions exhibit different physicochemical properties. We noted that Li(FS-NFS)I sample at concentrations of 7 and 10 m after cooling from the molten state, underwent solidification, solidification upon cooling from the molten state, and attained a gel state at room temperature. Within the SAXS profile (figure 1(c)), an additional Peak c was identified, corresponding to the interatomic distance between either the same anion or neighboring anions [1]. Additionally, Peak b exhibits an observable positive shift as the concentration increased, suggesting the diminishing of averaged spacing between (FS-NFS)I-networks.

We summarized the relationship between d-spacing and concentration in different salt solutions to study the effect of chain length on the solvation structure size (figure 2). The d-spacing for Peak a and Peak b can be calculated using the formula $d = 2\pi/q$. As the chain length increases, the d-spacing values of Peak a and Peak b also increase. The smaller d-spacing observed for Peak a and Peak b in Li(FS-FS)I solutions can be attributed to the smaller size of the anions since the formation of these two Peaks primarily arises from the anion network. In addition, we noticed an obvious d-spacing drop of Peak b in Li(FS-NFS)I solutions as concentration increases, indicating that the anion networks become increasingly crowded in large molecular weight salt solutions.

To provide additional evidence for our interpretation, we analyzed the correlation between the d-spacing and the carbon number of different imide-based anions. Specifically, the d-spacing of Peak a was plotted against the carbon numbers at concentrations of 1 m, 5 m, 10 m, and 15 m, as depicted in figure 3(a). The results demonstrate a positive correlation between the evolution of d-spacing and the number of carbons present in the fluorocarbon chains of the imide-based anions. This finding aligns with our previous results obtained for symmetric lithium imide salts [21]. The relationship between the d-spacing and concentration is illustrated in figure 3(b). The

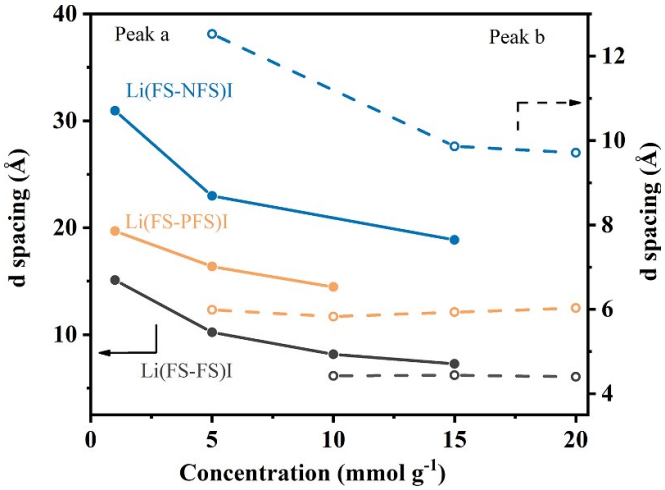

Figure 2. d-spacing of Peak a and Peak b is plotted as a function of concentrations in Li(FS-FS)I, (b) Li(FS-PFS)I, and Li(FS-NFS)I aqueous solutions.

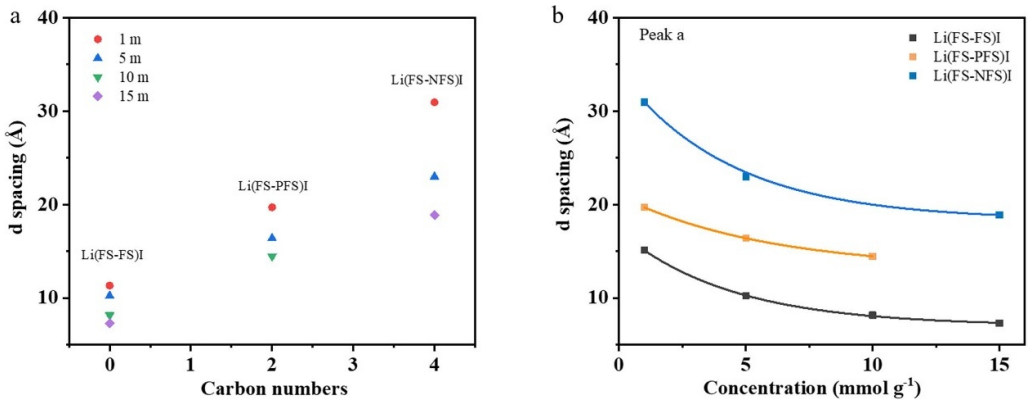

Figure 3. (a) d-spacing of Peak a as a function of carbon numbers at different concentrations. (b) d-spacing changes of Peak a as a function of concentration in Li(FS-FS)I, (b) Li(FS-PFS)I, and Li(FS-NFS)I aqueous solutions.

results indicate an exponential decrease in the d-spacing as a function of concentration, with the fitting parameters provided in table S1.

3.2. Raman results

To elucidate the solvation structures, Raman analysis was performed at ambient temperature for aqueous electrolytes such as Li(FS-FS)I, Li(FS-PFS)I, and Li(FS-NFS)I at varying concentrations, as shown in figures 4(a)–(c). In general, the intense band that appears at about 720–780 cm^{-1} represents the S-N-S bending vibration of the anions [30, 31]. As the electrolyte concentration increased from 0.5 to 20 m, the bending vibration (S-N-S) experienced a shift towards higher frequencies. This blue shift is associated with alterations in the electron density of the anion and the coordination structure between the cation and anion. The elevated number of the withdrawing electron groups (CF_3) reduces the Coulomb interaction between anion and Li^+ cation [32], leading to a smaller peak shift in the S-N-S vibrational mode of Li(FS-PFS)I (744–750 cm^{-1}) and Li(FS-NFS)I (732–736 cm^{-1}) compared to LiFSI (745–756 cm^{-1}). According to previous reports [33], there are three types of bending vibration of anions in aqueous solutions originating from (i) solvent-separated ion pairs (SSIPs), contacted ion pairs (CIPs), and aggregate ions (AGGs). Curve fitting was performed to separate each band and the fitting results are illustrated in figures 4(d) and (e) for Li(FS-FS)I and Li(FS-PFS)I aqueous solution. At low concentrations, the proportion of SSIPs in Li(FS-PFS)I aqueous solution surpasses that in Li(FS-FS)I, indicating the weaker interaction between cation and anion with increasing CF_3 groups. However, at higher concentrations, SSIPs in Li(FS-PFS)I aqueous solution form 15 m disappears, while they still account for approximately 15% in Li(FS-FS)I solution. Hence, the electrophilic properties and the geometric size may play pivotal roles in influencing the solvation structure of asymmetric Li salts in water. Due to the subtle differences in the S-N-S vibrational mode and the distinct configurations of the $(FS\text{-}PFS)I^-$ anion, an intricate overlap occurs among the peak of SSIPs, CIPs and AGGs [34]. This intricate interplay complicates the precise determination of the fractions of SSIPs, CIPs, and AGGs.

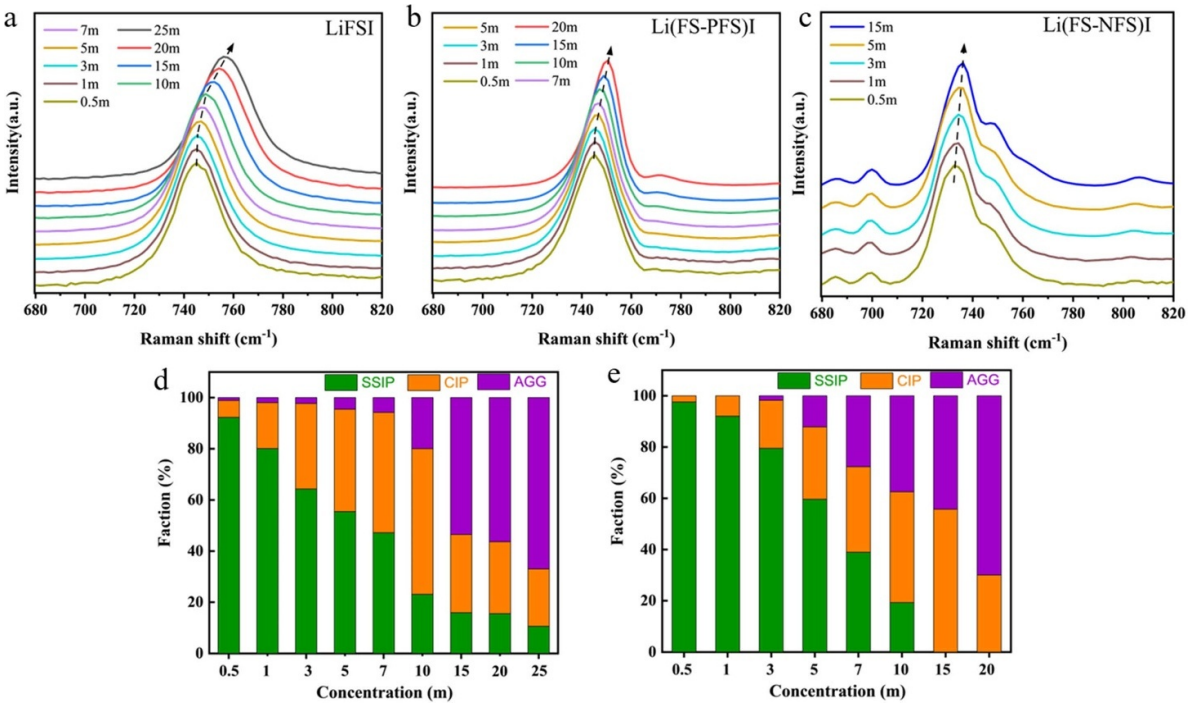

Figure 4. Raman analysis of (a) Li(FS-FS)I, (b) Li(FS-PFS)I, and (c) Li(FS-NFS)I aqueous solutions with different concentrations. SSIPs, CIPs and AGGs d of (d) Li(FS-FS)I, (e) Li(FS-PFS)I at different concentrations.

4. Conclusions

We investigated the physicochemical properties of imide-based asymmetric lithium salts with different concentrations in water. The SAXS spectra show the blue shifts of the lower q peak with decreased intensity as the increasing of concentration, indicating a decrease in the average distance between solvated anions. The increase in the population of anions and reduction of water molecules in highly concentrated solution induce the formation of FSI networks, which is indicated by the formation of additional peak at higher q value. Significantly, an exponential decrease in the d-spacing as a function of concentration was observed. In addition, we also applied the Raman spectroscopy technique to study the evolutions of solvent-separated ion pairs (SSIPs), contacted ion pairs (CIPs), and aggregate ions (AGGs) in the solvation structure of asymmetric salt solutions. The results obtained in this work benefit the understanding of the solvation structure of WISs electrolytes and promote the development of high-energy density batteries.

Data availability statement

All data that support the findings of this study are included within the article (and any supplementary files).

Acknowledgments

This research used resources of the Advanced Photon Source, a U.S. Department of Energy (DOE) Office of Science User Facility operated for the DOE Office of Science by the Argonne National Laboratory under Contract No. AC02-06CH11357. T Li is thankful for the support by the U.S. National Science Foundation (Grant Nos. 2208972, 2120559 and 2323117). T Li and H Nguyen acknowledge the support by the U. S. Department of Energy, Office of Energy Efficiency and Renewable Energy, Vehicle Technologies Office.

ORCID iD

Lingzhe Fang https://orcid.org/0000-0001-9243-7741

References

[1] Gordon D, Wu M Y, Ramanujapuram A, Benson J, Lee J T, Magasinski A, Nitta N, Huang C and Yushin G 2016 Enhancing cycle stability of lithium iron phosphate in aqueous electrolytes by increasing electrolyte molarity *Adv. Energy Mater.* **6** 1501805

[2] Zheng J *et al* 2018 Understanding thermodynamic and kinetic contributions in expanding the stability window of aqueous electrolytes *Chem* **4** 2872–82

[3] Shen Y, Liu B, Liu X, Liu J, Ding J, Zhong C and Hu W 2021 Water-in-salt electrolyte for safe and high-energy aqueous battery *Energy Storage Mater.* **34** 461–74

[4] Suo L *et al* 2016 Advanced high-voltage aqueous lithium-ion battery enabled by "water-in-bisalt" electrolyte *Angew. Chem., Int. Ed. Engl.* **55** 7136–41

[5] Suo L, Han F, Fan X, Liu H, Xu K and Wang C 2016 "Water-in-salt" electrolytes enable green and safe Li-ion batteries for large scale electric energy storage applications *J. Mater. Chem.* A **4** 6639–44

[6] Lukatskaya M R, Feldblyum J I, Mackanic D G, Lissel F, Michels D L, Cui Y and Bao Z 2018 Concentrated mixed cation acetate "water-in-salt" solutions as green and

low-cost high voltage electrolytes for aqueous batteries *Energy Environ. Sci.* **11** 2876–83
[7] Li C Y, Chen M, Liu S, Lu X, Meng J, Yan J, Abruna H D, Feng G and Lian T 2022 Unconventional interfacial water structure of highly concentrated aqueous electrolytes at negative electrode polarizations *Nat. Commun.* **13** 5330
[8] Suo L, Borodin O, Gao T, Olguin M, Ho J, Fan X, Luo C, Wang C and Xu K 2015 "Water-in-salt" electrolyte enables high-voltage aqueous lithium-ion chemistries *Science* **350** 6266
[9] Ding M S, von Cresce A and Xu K 2017 Conductivity, viscosity, and their correlation of a super-concentrated aqueous electrolyte *J. Phys. Chem.* C **121** 2149–53
[10] Borodin O, Self J, Persson K A, Wang C and Xu K 2020 Uncharted waters: super-concentrated electrolytes *Joule* **4** 69–100
[11] Lim J, Park K, Lee H, Kim J, Kwak K and Cho M 2018 Nanometric water channels in water-in-salt lithium ion battery electrolyte *J. Am. Chem. Soc.* **140** 15661–7
[12] Jeon J and Cho M 2021 Ion transport in super-concentrated aqueous electrolytes for lithium-ion batteries *J. Phys. Chem.* C **125** 23622–33
[13] Dubouis N, Lemaire P, Mirvaux B, Salager E, Deschamps M and Grimaud A 2018 The role of the hydrogen evolution reaction in the solid–electrolyte interphase formation mechanism for "water-in-salt" electrolytes *Energy Environ. Sci.* **11** 3491–9
[14] Wang F *et al* 2018 Hybrid aqueous/non-aqueous electrolyte for safe and high-energy Li-ion batteries *Joule* **2** 927–37
[15] Chen L *et al* 2020 A 63 m superconcentrated aqueous electrolyte for high-energy Li-ion batteries *ACS Energy Lett.* **5** 968–74
[16] Wang F, Sun Y and Cheng J 2023 Switching of redox levels leads to high reductive stability in water-in-salt electrolytes *J. Am. Chem. Soc.* **145** 4056–64
[17] Gao H, Tang K, Xiao J, Guo X, Chen W, Liu H and Wang G 2022 Recent advances in "water in salt" electrolytes for aqueous rechargeable monovalent-ion (Li^+, Na^+, K^+) batteries *J. Energy Chem.* **69** 84–99
[18] Han J, Mariani A, Passerini S and Varzi A 2023 A perspective on the role of anions in highly concentrated aqueous electrolytes *Energy Environ. Sci.* **16** 1480–501
[19] Liu X, Lee S-C, Seifer S, Winans R E, Cheng L, Y Z and Li T 2022 Insight into the nanostructure of "water in salt" solutions: a SAXS/WAXS study on imide-based lithium salts aqueous solutions *Energy Storage Mater.* **45** 696–703
[20] Yamada Y, Usui K, Sodeyama K, Ko S, Tateyama Y and Yamada A 2016 Hydrate-melt electrolytes for high-energy-density aqueous batteries *Nat. Energy* **1** 16129
[21] Liu X, Yu Z, Sarnello E, Qian K, Seifert S, Winans R E, Cheng L and Li T 2021 Microscopic understanding of the ionic networks of "water-in-salt" electrolytes *Energy Mater. Adv.* **2021** 7368420
[22] Ko S, Yamada Y, Miyazaki K, Shimada T, Watanabe E, Tateyama Y, Kamiya T, Honda T, Akikusa J and Yamada A 2019 Lithium-salt monohydrate melt: a stable electrolyte for aqueous lithium-ion batteries *Electrochem. Commun.* **104** 106488
[23] Becker M, Kuhnel R S and Battaglia C 2019 Water-in-salt electrolytes for aqueous lithium-ion batteries with liquidus temperatures below −10 °C *Chem. Commun.* **55** 12032–5
[24] Reber D, Kühnel R-S and Battaglia C 2019 Suppressing crystallization of water-in-salt electrolytes by asymmetric anions enables low-temperature operation of high-voltage aqueous batteries *ACS Mater. Lett.* **1** 44–51
[25] Zhang Y *et al* 2021 *J. ACS Energy Lett.* **6** 3458–63
[26] Qian K, Winans R E and Li T 2021 Insights into the nanostructure, solvation, and dynamics of liquid electrolytes through small-angle x-ray scattering *Adv. Energy Mater.* **11** 2002821
[27] Lyu Y, Wang H, Liu X, He L, Do C, Seifert S, Winans R E, Cheng L and Li T 2024 Solvation structure of methanol-in-salt electrolyte revealed by small-angle x-ray scattering and simulations *ACS Nano* **18** 7037–45
[28] Liu X, Fang L, Lyu X, Winans R E and Li T 2023 Unveiling the liquid electrolyte solvation structure by small angle x-ray scattering *Chem. Mater.* **35** 9821–32
[29] Zhang Y *et al* 2021 Water-in-salt LiTFSI aqueous electrolytes. 1. Liquid structure from combined molecular dynamics simulation and experimental studies *J. Phys. Chem.* B **125** 4501–13
[30] Suo L *et al* 2017 How solid-electrolyte interphase forms in aqueous electrolytes *J. Am. Chem. Soc.* **139** 18670–80
[31] Han S-D, Sommer R D, Boyle P D, Zhou Z-B, Young V G, Borodin O and Henderson W A 2022 Electrolyte solvation and ionic association: part IX. Structures and Raman spectroscopic characterization of LiFSI solvates *J. Electrochem. Soc.* **169** 110544
[32] O'Connor M J, Boblak K N, Topinka M J, Kindelin P J, Briski J M, Zheng C and Klumpp D A 2010 Superelectrophiles and the effects of trifluoromethvl substituents *J. Am. Chem. Soc.* **132** 3266–7
[33] Liu X, Lee S C, Seifert S, He L, Do C, Winans R E, Kwon G, Zhang Y and Li T 2023 Revealing the correlation between the solvation structures and the transport properties of water-in-salt electrolytes *Chem. Mater.* **35** 2088–94
[34] Karuppasamy K, Vikraman D, Hwang I-T, Kim H-J, Nichelson A, Bose R and Kim H-S 2020 Nonaqueous liquid electrolytes based on novel 1-ethyl-3-methylimidazolium bis(nonafluorobutane-1-sulfonyl imidate) ionic liquid for energy storage devices *J. Mater. Res. Technol.* **9** 1251–60